

# Lawrence Berkeley National Laboratory

## Recent Work

### Title

Identification and characterization of two energy gaps in superconducting MgB<sub>2</sub> by specific-heat measurements

### Permalink

<https://escholarship.org/uc/item/0f31q91q>

### Authors

Fisher, R.A.  
Bouquet, F.  
Phillips, N.E.  
et al.

### Publication Date

2001-09-01

# Specific Heat of Mg<sup>11</sup>B<sub>2</sub>

F. Bouquet,<sup>1</sup> R. A. Fisher,<sup>1</sup> N. E. Phillips,<sup>1</sup> D. G. Hinks,<sup>2</sup> and J. D. Jorgensen<sup>2</sup>

<sup>1</sup>*Lawrence Berkeley National Laboratory and Department of Chemistry, University of California, Berkeley, CA 94720*

<sup>2</sup>*Materials Science Division, Argonne National Laboratory, Argonne, IL 60439*

(Dated: April 11, 2001)

Measurements of the specific heat of Mg<sup>11</sup>B<sub>2</sub>, from 1 to 50 K, in magnetic fields to 9 T, give the Debye temperature,  $\Theta = 1050$  K, the coefficient of the normal-state electron contribution,  $\gamma_n = 2.6$  mJ mol<sup>-1</sup> K<sup>-2</sup>, and a discontinuity in the zero-field specific heat of 133 mJ mol<sup>-1</sup> K<sup>-1</sup> at  $T_c = 38.7$  K. The estimated value of the electron-phonon coupling parameter,  $\lambda = 0.62$ , could account for the observed  $T_c$  only if the important phonon frequencies are unusually high relative to  $\Theta$ . At low  $T$ , there is a strongly field-dependent feature that suggests the existence of a second energy gap, about four times smaller than the major gap.

PACS numbers: 74.25.Bt, 74.60.Ec, 75.40.Cx

The superconductivity of MgB<sub>2</sub>, with  $T_c = 39$  K [1] and an isotope effect [2, 3, 4] consistent with the phonon-mediated electron pairing of the BCS theory [5], has reopened the question of the maximum  $T_c$  that can be produced by that mechanism [6, 7]. It also raises the complementary question: What is the mechanism of the superconductivity of MgB<sub>2</sub> itself? In this Letter, we report measurements of the heat capacity ( $C$ ) of Mg<sup>11</sup>B<sub>2</sub> that give information relevant to the latter question: Comparison of the coefficient ( $\gamma_n$ ) of the normal-state electron contribution to  $C$  with band-structure calculations [8, 9, 10] gives an estimate of the electron-phonon coupling parameter ( $\lambda$ ). The value of  $\lambda$  suggests moderately strong coupling, but whether it can account for the high value of  $T_c$  on the basis of phonon coupling alone depends on the values of other parameters that are not yet determined. In the superconducting state  $C$  deviates from the BCS expression in a way that has no parallel among known superconductors, and which suggests the presence of a second, smaller gap in the electron density of states (EDOS), which has a non-BCS dependence on  $T$ .

The Mg<sup>11</sup>B<sub>2</sub> sample was a powder, prepared by reacting <sup>11</sup>B powder and Mg metal in a capped BN crucible at 850°C under a 50-bar argon atmosphere for 1.5 hours. Thermal contact to the powder was achieved by mixing it with a small amount of GE7031 varnish (a common low- $T$  thermal contact agent with a known heat capacity) in a thin-walled copper cup. These extra contributions to the addenda limited the precision of the data. However, the alternate method of providing thermal contact, sintering the powder, can have adverse effects on the sample [11] and may in some cases account for differences between the results reported here and those obtained in other measurements. The measurements of  $C$  were made by a modified heat-pulse technique, 1–32 K, and by a continuous-heating technique, 29–50 K. Measurements in magnetic field ( $H$ ) were made on the field-cooled (FC) sample after applying the field at  $T \geq 60$  K. For  $H = 1$

T, for which the field penetration is about 50% of that in the normal state, measurements made after applying the field at 1 K were indistinguishable from the FC results, suggesting that equilibrium flux distributions were attained.

Below 2 K, there is an  $H$ -dependent hyperfine contribution to  $C$ . There are also several  $H$ -independent features in  $C$ , including an “upturn” below 2 K, that are probably associated with small amounts of impurity phases (or possibly with the GE varnish, although past experience makes that seem unlikely). Partly for that reason, most of the interpretation of the results is based on an analysis of the differences,  $C(H) - C(9$  T), in which the  $H$ -independent extraneous contributions and most of the contributions of the addenda, including the varnish, cancel.  $C(H) - C(9$  T) was calculated after the data were corrected for the hyperfine contributions and a small  $H$ -dependent part of the heat capacity of the sample holder. Since  $C$  is the sum of an  $H$ -dependent electron contribution ( $C_e$ ) and an  $H$ -independent lattice contribution ( $C_l$ ), an analysis of  $C(H) - C(9$  T) also has the advantage that  $C_l$  cancels, leaving  $C_e(H)$ , the contribution of greater interest. In the normal state  $C_e(H) = \gamma_n T$ , independent of  $H$ ; in the mixed state  $C_e(H)$  includes a  $T$ -proportional term,  $\gamma(H)T$ , and  $H$ -dependent terms; in the superconducting state,  $C_e(0) = C_{es}$ .

The upper critical field ( $H_{c2}$ ) of MgB<sub>2</sub> is approximately linear in  $T$  with  $H_{c2}(0) \sim 16$  T [12]. This is reasonably consistent with the  $C$  measurements, for which the onset of the transition to the mixed state, at  $H = H_{c2}(T)$ , is marked by the deviations of  $C(H) - C(9$  T) from zero (see Fig 1(a)). It leads to the expectation that for 9 T the sample would be in the normal state for  $T \geq 20$  K. The data actually plotted in Fig. 1(a) are the differences,  $[C(H) - C(9$  T)]/ $T$ , but with the scale shifted by  $\gamma(9$  T). (They are essentially point-to-point differences, with no smoothing of the 9-T data, which increases the scatter.) The values of  $\gamma(H)$  have been determined by fit-

ting the low- $T$ , mixed- and superconducting-state data with  $[C(H) - C(9\text{ T})] = [\gamma(H) - \gamma(9\text{ T})]T + a \exp(-b/T)$ , where  $a$  and  $b$  are  $H$  dependent. Consistent with the  $H = 0$  data,  $\gamma(0)$  was taken as zero, fixing the values of  $\gamma(H)$  for all  $H$ . Figure 2 shows  $\gamma(H)$  vs  $H$ , and the extrapolation to  $H_{c2}(0) = 16\text{ T}$  to obtain  $\gamma_n = 2.6\text{ mJ mol}^{-1}\text{ K}^{-2}$ . Although the extrapolation is somewhat arbitrary, the very small differences between  $\gamma(5\text{ T})$ ,  $\gamma(7\text{ T})$ , and  $\gamma(9\text{ T})$  suggest that it gives  $\gamma_n$  to within  $\sim 0.1\text{ mJ mol}^{-1}\text{ K}^{-2}$ . If the sample were normal at all temperatures in 9 T the quantity shown in Fig. 1(a) would be exactly  $C_e(H)/T$ . That is not the case, but the differences are small, as shown by the small differences between  $C(5\text{ T})$ ,  $C(7\text{ T})$ , and  $C(9\text{ T})$ . Quantitatively,  $C_e(H)/T$  is underestimated by the amount  $\gamma_n - C_e(9\text{ T})/T$ . For  $T \leq 10\text{ K}$ ,  $\gamma_n - C_e(9\text{ T})/T \approx \gamma_n - \gamma(9\text{ T}) \approx 0.08\text{ mJ mol}^{-1}\text{ K}^{-2}$ ; for  $10 \leq T \leq 20\text{ K}$ , where there must be a small broad anomaly in  $C(9\text{ T})$ , the underestimate is smaller and  $T$ -dependent.

The transition to the superconducting state, shown in Fig. 1(c), with an entropy-conserving construction that gives  $T_c = 38.7\text{ K}$  and  $\Delta C(T_c) = 133\text{ mJ mol}^{-1}\text{ K}^{-1}$ , is relatively sharp, with a width  $\sim 2\text{ K}$ . In this temperature interval the sample is in the normal state for  $H = 9\text{ T}$ , and addition of  $\gamma_n = 2.6\text{ mJ mol}^{-1}\text{ K}^{-2}$  to the quantity plotted would give the electron contribution to  $C$  through the transition. The effect of  $H$  in broadening the transition (to the mixed state), as expected for measurements on a powder with an anisotropic  $H_{c2}$  [9, 13], is evident in Fig. 1(a).

The thermodynamic consistency of the data, including in particular the very unusual  $T$  dependence of  $C_{es}(0)$ , can be tested by calculating the difference in entropy ( $S$ ) between 0 and  $T_c$  for different fields. The result of such a test is shown in Fig. 3(a) where the entropies obtained by integrating the plotted points are compared with  $\gamma(9\text{ T})T$ , which represents the 9 T data. At 40 K, the entropies for all  $H$  are within  $\pm 2\%$  of the same value. The result of a second integration of the entropies to obtain free energy differences and the thermodynamic critical field ( $H_c$ ) is shown in Fig. 3(b).

Fitting the 9-T data for  $20 \leq T \leq 50\text{ K}$  with  $C(9\text{ T}) = \gamma_n T + C_l$ , where  $C_l = B_3 T^3 + B_5 T^5$ , gave  $B_3 = 5.1 \times 10^{-3}\text{ mJ mol}^{-1}\text{ K}^{-4}$  and  $B_5 = 2.5 \times 10^{-6}\text{ mJ mol}^{-1}\text{ K}^{-6}$ . The Debye temperature ( $\Theta$ ), calculated following the usual convention of using the value of  $B_3$  per g atom, is  $1050 \pm 50\text{ K}$ .

Fig. 1(a) includes a comparison of the experimental  $C_{es}$  with that for a BCS superconductor with  $\gamma_n = 2.6\text{ mJ mol}^{-1}\text{ K}^{-2}$  and  $T_c = 38.7\text{ K}$ . For  $T \geq 27\text{ K}$ ,  $C_{es}$  is approximately parallel to the BCS curve; at lower  $T$  it rises above the BCS curve and then decreases to zero as  $a \exp(-b/T)$ , but with values of  $a$  and  $b$  very different from those of the BCS superconductor. It seems unlikely that this behavior could be understood on the basis of gap anisotropy similar to that known in other superconductors. Qualitatively, it gives the appearance of a transition to the superconducting state in two stages: the

first, a partial transition at  $T_c$  that leaves a “residual”  $\gamma$  (the extrapolation of  $C_{es}$  to  $T = 0$  from above 12 K gives  $\sim 1\text{ mJ mol}^{-1}\text{ K}^{-2}$ , but it should be regarded as an overestimate because it does not allow for the full entropy associated with the second stage); a second stage that is associated with a second, smaller, energy gap, which decreases in amplitude in the vicinity of 10 K. Taking the exponential decrease in  $C_{es}$  as a manifestation of a BCS-like transition, and comparing the parameters  $a$  and  $b$  with BCS theory, gives  $T_c = 11\text{ K}$  and  $\gamma = 0.74\text{ mJ mol}^{-1}\text{ K}^{-2}$ . This interpretation of  $C_{es}$  is, to some degree, understandable on the basis of theoretical considerations: It has been suggested that the gaps may be different on two parts of the Fermi surface [14], and, depending on the strength of the electron-phonon coupling between, and on, the two parts, the amplitude of the small gap can show a relatively abrupt decrease at a temperature well below  $T_c$ . Although both gaps open at  $T_c$ , that feature in the small gap could produce the observed feature in  $C_{es}$  in the 8–12 K region. The existence of two gaps on the Fermi surface is also consistent with scanning tunneling spectroscopy, which has shown both a flat-bottomed BCS-like gap at low  $T$ , but with a small amplitude,  $\sim 2\text{ meV}$ , corresponding to a BCS  $T_c$  of  $\sim 13\text{ K}$  [15], and a V-shaped gap with an amplitude of  $\sim 5.2\text{ meV}$ , corresponding to a BCS  $T_c$  of 35 K [16], more compatible with the observed  $T_c$ . Despite the difficulty of explaining why and how different groups measure different gaps (see also [17] and [18]), it is striking how well these two gaps would account for  $C_{es}$ : At low  $T$ , where the thermal excitations are too weak to overcome the larger gap, the exponential behavior of  $C_{es}$  is consistent with the smaller gap; the opening of the large gap at  $T_c$  explains the large  $\Delta C(T_c)$ . Moreover, between 20 K and  $T_c$ ,  $C_{es}/T$  has a linear behavior (see Fig. 1(a)), which is consistent with a V-shaped gap. (Similar  $T^2$  behavior has been seen in heavy-fermion superconductors [19].)

Anisotropy in  $H_{c2}$  cannot explain the dramatic increase in  $\gamma(H)$  at low  $H$  shown in Fig. 2. The dashed curve is a calculation using the effective-mass model with an anisotropy of 10, which is already greater than reported values [9, 13], but  $\gamma(H)$  cannot be fitted with *any* value of the anisotropy. The rapid increase in  $\gamma(H)$  at low  $H$  reflects the difference between  $C_e(0.5\text{ T})$  and  $C_e(0)$  below 10 K, and is related to the existence of the second gap.

An average over the Fermi surface of the electron-phonon coupling parameter can be estimated by comparing  $\gamma_n$  with band-structure calculations of the “bare” EDOS at the Fermi surface ( $N(0)$ ) using the relation  $\gamma_n = (1/3)\pi^2 k_B^2 N(0)(1 + \lambda)$ .  $N(0)$  has been reported as 0.68, 0.71, and 0.72 states  $\text{eV}^{-1}\text{ unit cell}^{-1}$  (Refs. [8], [9], and [10] respectively) giving  $\lambda = 0.62, 0.56, \text{ and } 0.53$ . Theoretically calculated values of  $\lambda$  are 0.68 [8], and  $\sim 1$  [10]. In the Mc Millan relation [6],  $T_c$  is related to  $\lambda, \Theta$ ,

and the electron–electron repulsion ( $\mu^*$ ) by

$$T_c = (\Theta/1.45) \exp\{-1.04(1 + \lambda)/[\lambda - \mu^*(1 + 0.62\lambda)]\}, \quad (1)$$

with  $\mu^*$  frequently taken to be  $\sim 0.1$  [6, 7]. With  $\lambda = 0.62$ , the highest of the values derived from  $\gamma_n$  and  $N(0)$ , and  $\Theta = 1050$  K Eq. (1) gives  $T_c = 22$  K, too low by almost a factor two. With these values of  $\lambda$  and  $\Theta$ ,  $T_c = 39$  K would require  $\mu^* = 0.030$ , an unusually low value. However, in this expression  $\Theta$  represents a relatively crude estimate of the phonon frequencies that are important in the electron pairing. As derived from the coefficient of the  $T^3$  term in  $C_l$ ,  $\Theta$  is really a measure of the frequencies of the low–frequency acoustic phonons, which may not be particularly relevant to the pairing of the electrons. In the Debye model,  $\Theta$  is also the cut–off frequency, but real phonon spectra often extend to significantly higher frequencies. In the Allen and Dynes version of the theory [7],  $\Theta/1.45$  is replaced by  $\omega_{log}/1.20$ , where  $\omega_{log}$  is a moment of the phonon frequencies in which they are weighted by the electron–phonon matrix elements. More detailed calculations that take into account relevant features of the phonon spectrum and electron–phonon scattering may give a value of the pre–exponential factor in Eq. (1) that accounts for the observed  $T_c$  with a physically plausible value of  $\mu^*$ , but until they are available, the question of whether the electron pairing in MgB<sub>2</sub> is phonon mediated would seem to remain open.

The parameters  $(H_c(0))^2/\gamma_n T_c^2$  and  $\Delta C(T_c)/\gamma_n T_c$  measure the strength of the electron pairing [20]. In the BCS, weak–coupling limit, their values are 5.95 and 1.43, respectively. There are a number of “strong–coupled” superconductors for which these parameters are greater than the BCS values, but relatively few for which they are smaller [20]. For Mg<sup>11</sup>B<sub>2</sub> they are unusually small, 5.46 and 1.32, which, in contrast with the value of  $\lambda$ , suggests extreme weak coupling. This indication of weak coupling, based on bulk properties, is in qualitative agreement with tunneling results that may have been influenced by surface effects [16].

In general, there are more differences than similarities among the specific heat measurements on MgB<sub>2</sub> [2, 21, 22, 23, 24]. However, in several important respects, including the low– $T$  behavior of  $C_{es}$ , the results of the Geneva group [21] are qualitatively similar to those reported here, and the differences that do occur are readily understood in terms of sample dependence. A comparison with their results, which were obtained by different experimental techniques on sintered sample of commercial material, attests the qualitative validity of the major features reported both here and in Ref. [21]: The value of  $\gamma_n$ , 2.7 mJ mol<sup>−1</sup> K<sup>−2</sup>, and the test of thermodynamic consistency in Ref. [21] are similar and of comparable accuracy to those reported here, but limited by paramagnetic Fe impurities in Ref. [21] and the precision of the data here. Although the superconducting–state entropies are essentially identical at  $T_c$ , the specific

heat anomaly at  $T_c$  in Ref. [21] is broader, leading to a substantial underestimate of  $\Delta C(T_c)$ . Most importantly, the  $T$ –dependence of  $C_{es}$  in the 4–15 K range, which shows the presence of a second gap (or extreme an unusual anisotropy), is essentially the same in both cases. However, for  $T \leq 4$  K,  $C_{es}$  was obscured by the contribution of paramagnetic impurities and the limiting  $T \rightarrow 0$  dependence was taken as approximately  $T^2$  [21], which would be expected for line nodes, rather than the exponential dependence reported here.

Several other values of  $\Delta C(T_c)$ , all for sintered samples and all lower than that reported here, have been given in other reports [2, 22, 23, 24]. Values of  $\gamma_n$  that range from 1.1 to 5.5 mJ mol<sup>−1</sup> K<sup>−2</sup>, based on different [22, 24] or unspecified [2] analysis of experimental data have also been reported, but the very similar values reported here and in Ref. [21], are supported by the thermodynamic consistency of the data

We have benefited from useful discussions with J. M. An, M. L. Cohen, G. W. Crabtree, J. P. Franck, R. A. Klemm, C. Marcenat, I. I. Mazin, and W. E. Pickett. The work at LBNL was supported by the Director, Office of Basic Energy Sciences, Materials Sciences Division of the U. S. DOE under Contract No. DE–AC03–76SF00098. The work at ANL was supported by the U. S. DOE, BS–MS under Contract No. W–31–109–ENG–38.

## REFERENCES

- [1] J. Nagamatsu *et al.*, Nature **410**, 63 (2001).  
 [2] S. L. Bud'ko *et al.*, Phys. Rev. Lett. **86**, 1877 (2001).  
 [3] D. G. Hinks, H. Claus, and J. D. Jorgensen, to be published.  
 [4] D. D. Lawrie, J. P. Franck, and G. Zhang, to be published.  
 [5] J. Bardeen, L. N. Cooper, and J. R. Schrieffer, Phys. Rev. **108**, 1175 (1957).  
 [6] W. L. McMillan, Phys. Rev. **167**, 331 (1968).  
 [7] P. B. Allen and R. C. Dynes, Phys. Rev. B **12**, 905 (1975).  
 [8] H. Sun, D. Roundy, H. J. Choi, S. G. Louie, M. L. Cohen, to be published.  
 [9] J. M. An, and W. E. Pickett, cond-mat/0102391 (2001).  
 [10] J. Kortus *et al.*, cond-mat/0101446v2 (2001).  
 [11] J. P. Franck, private communication.  
 [12] S. L. Bud'ko *et al.*, cond-mat/0102413v2 (2001).  
 [13] O. F. de Lima *et al.*, cond-mat/0103287v3 (2001).  
 [14] A. Y. Liu, J. Kortus, and I. L. Mazin, to be published.  
 [15] G. Rubio-Bollinger, H. Suderow, and S. Vieira, cond-mat/0102242 (2001).  
 [16] G. Karapetrov *et al.*, cond-mat/0102312 (2001).  
 [17] H. Schmidt *et al.*, cond-mat/0102389 (2001).  
 [18] A. Sharoni, I. Felner, and O. Millo, cond-mat/0102325v3 (2001).  
 [19] R. A. Fisher *et al.*, Phys. Rev. Lett. **62**, 1411 (1989).  
 [20] H. Padamasee *et al.*, J. Low Temp. Phys. **12**, 387 (1973).  
 [21] Y. Wang, T. Plackowski, and A. Junod, cond-mat/0103181 (2001).  
 [22] R. K. Kremer, B. J. Gibson, and K. Ahn, cond-mat/0102432 (2001).  
 [23] C. Marcenat, A. Pautrat, D. D. Lawrie, J. P. Franck, and G. Zhang, to be published.  
 [24] Ch. Wälti *et al.*, cond-mat/0102522v3 (2001).

FIG. 1: (a)  $[C(H) - C(9\text{ T})]/T$ . In (a) and (b) the scale has been shifted by  $\gamma(9\text{ T})$  to give an approximation to  $C_e(H)/T$  (see text). In (a) the dashed curve is a polynomial extrapolation of the 12–20 K,  $H = 0$  data to  $T = 0$ ; the horizontal line represents  $\gamma(9\text{ T})$ . In (b) the low- $T$  5- and 7-T data are shown on an expanded scale with solid curves representing fits described in the text; the horizontal solid and dashed lines represent  $\gamma(9\text{ T})$  and  $\gamma_n$ , respectively. In (c) the solid lines represent an entropy conserving construction. The error bars are  $\pm 0.1\% C_{total}/T$ .

FIG. 2:  $\gamma$  as a function of  $H$ . The solid curve is a guide to the eye and an extrapolation to  $H_{c2}(0)$ . The dashed curve is a “fit” with an  $H_{c2}$  anisotropy of 10.

FIG. 3: (a) Entropies as functions of  $T$  for different  $H$ , with  $H$  increasing from the lowest to highest curve. (b) Thermodynamic critical field, compared with a BCS curve for the derived values  $\gamma_n$  and  $T_c$ .

Figure 1

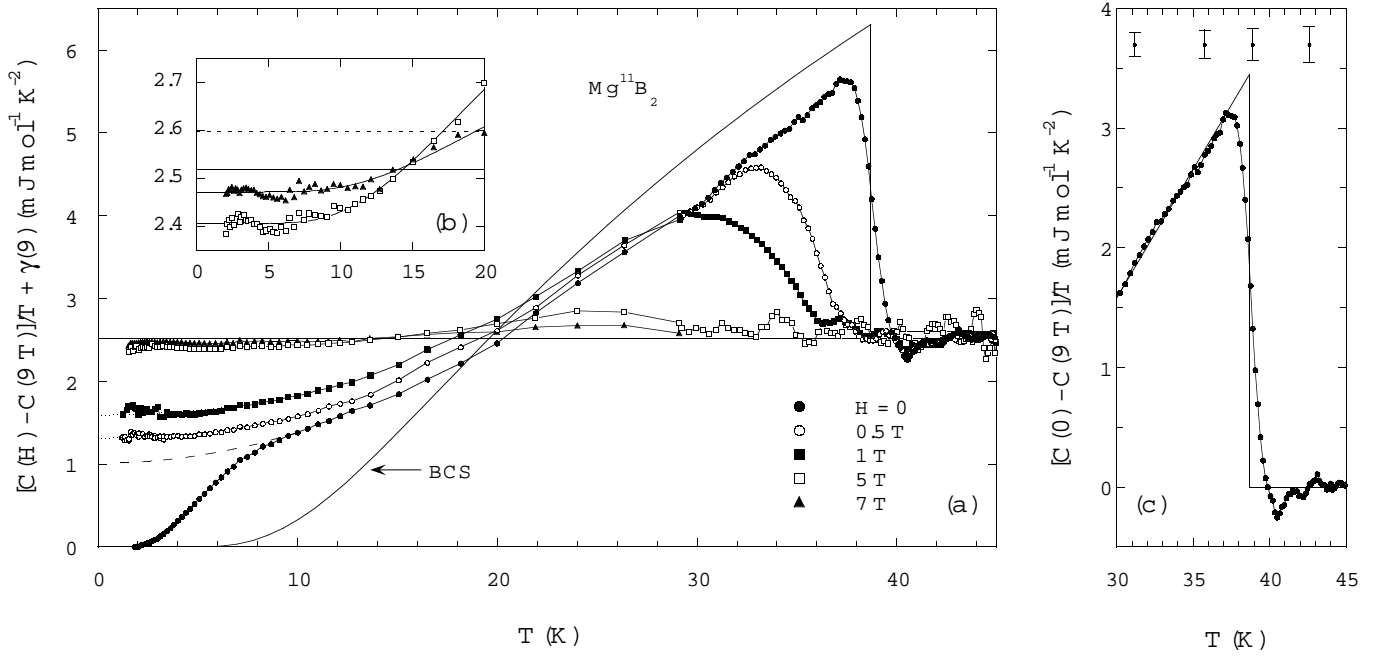


Figure 2

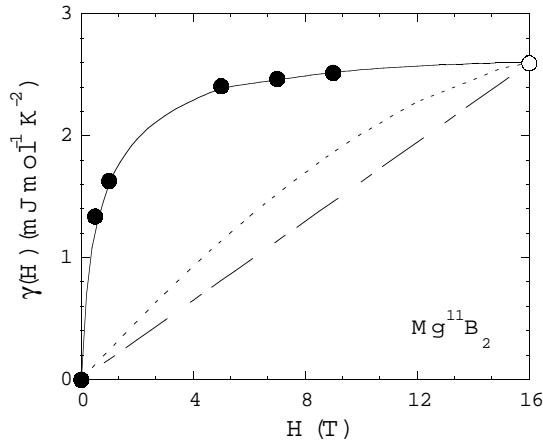


Figure 3

